

# Hybrid Triple-Junction Solar Cells by Surface Activate Bonding of III-V Double-Junction-Cell Heterostructures to Ion-Implantation-Based Si Cells

Naoteru Shigekawa<sup>1</sup>, Li Chai<sup>1</sup>, Masashi Morimoto<sup>1</sup>, Jianbo Liang<sup>1</sup>,  
Ryusuke Onitsuka<sup>2</sup>, Takaaki Agui<sup>2</sup>, Hiroyuki Juso<sup>2</sup>, and Tatsuya Takamoto<sup>2</sup>

<sup>1</sup>Osaka City University, 3-3-138 Sugimoto, Sumiyoshi, Osaka 558-8585, Japan

<sup>2</sup>Sharp Corp., 492 Minoshō, Yamatokoriyama, Nara 639-1186, Japan

**Abstract**—A hybrid triple-junction cell was fabricated by surface activated bonding of a lattice-matched invertedly-grown InGaP/GaAs double-junction cell to an ion-implantation-based Si bottom cell. An  $n^+$ -doped layer on the top of bottom cell due to the ion implantation worked as its emitter and bonding layer for the tunnel junction. The bonding interface was found to be stable after the annealing at 400 °C. An efficiency of 24.4% was achieved at air mass 1.5G and one sun at room temperature.

**Index Terms**—surface activated bonding, multi-junction cell, InGaP, GaAs, Si, bonding interface

## I. INTRODUCTION

Multi-junction solar cells made of III-V semiconductors are promising as practical candidate for next-generation high-efficiency solar cells [1]. Conversion efficiencies > 30% were reported for InGaP/InGaAs/Ge and InGaP/GaAs/InGaAs triple-junction cells [2], [3]. A conversion efficiency of 44.47% was achieved for InGaP/GaAs/InGaAsP/InGaAs four-junction cells [4].

Given that Si is the most popular semiconductor materials in photovoltaic industries, multi-junction cells should be fabricated on Si, i.e., Si cells should be used as their bottom cells. Several authors reported the growth of III-V based cells on Si [5]–[7]. However, III-V-on-Si multi-junction cells cannot be easily fabricated using crystal growth (monolithic approach) because of (1) the difference in lattice constants and thermal expansion coefficients between III-V materials and Si [8] and (2) the frequent appearance of the anti-phase domain [9].

Surface activated bonding (SAB) has been applied for fabricating junctions made of dissimilar materials (hybrid approach) since surfaces of samples are activated using Ar fast atom beams in high vacuum and samples are bonded without heating [10]–[15]. The electrical characteristics of SAB-based Si/Si, Si/GaAs, Si/InP and Si/GaN junctions were reported [13], [14], [16], [17]. There were reports on SAB-based InGaP/GaAs/Si hybrid triple-junction cells in which  $n$ -GaAs/ $n$ -Si isotype heterojunctions were employed for bonding. Conversion efficiencies of 20.5 (1 sun) and 23.6% (71 sun) were achieved [18].

We previously found that the band profile of SAB-based GaAs/Si junctions revealed type-II properties [19], which indicates that  $p$ -GaAs/ $n$ -Si junctions are preferable as tunnel junctions since the overlap of the bandgaps is effectively reduced. Furthermore we applied  $p$ -GaAs/ $n$ -Si tunnel junctions for InGaP/Si double-junction cells [20]. In this work,

we fabricated and characterized InGaP/GaAs/Si hybrid triple-junction cells by the surface activated bonding of invertedly-grown InGaP/GaAs double junction cell heterostructures to ion-implantation-based Si bottom cells. We also examined characteristics of the double-junction cells bonded to high-conductive Si substrates.

## II. RESULTS AND DISCUSSION

### A. Sample Preparation

We grew an  $n$ -on- $p$  lattice-matched double junction cell structure that was made of a buffer layer, a top contact layer, an InGaP-based top cell structure, a tunnel-junction layer, a GaAs-based bottom cell structure, and a GaAs bonding layer on a GaAs substrate. Note that the top-cell and bottom-cell structures were grown in the reverse order. We separately prepared an  $n^+$ -doped layer on the top of a high-resistive (100)  $p$ -Si substrate, which should work as the emitter and a part of the tunnel junction, by the implantation of phosphor (P) ions (acceleration energy:10 keV) and annealing (900 °C, 1 min.). The depth and height of the peak in the distribution profile of implanted P atoms after the annealing were estimated to be  $\approx 13$  nm and  $\sim 6 \times 10^{19}$  cm<sup>-3</sup>, respectively, by preparatory secondary ion mass spectroscopy measurements. We also formed a heavily  $p$ -doped layer on the backside of the Si substrate by the implantation of boron ions for achieving the electrical conduction.

The double-junction cell structure was bonded to the bottom cell structure by SAB. The GaAs substrate and the buffer layer were successively etched off so that the top contact layer was exposed. We then fabricated InGaP/GaAs/Si triple junction cells by using a conventional device process sequence, which was composed of (i) forming the emitter electrodes by AuGe/Ni/Au evaporation and annealing (400 °C, 1 min.), (ii) etching the top contact layer, (iii) etching the III-V layers for mesa isolation, (iv) depositing an anti-reflection film, (v) forming pads on the emitters, and (vi) forming the base contacts on the backside of bottom cells by evaporating an Al layer. The entire process flow and the schematic cross section of the fabricated triple junction cells are shown in Fig. 1. We also fabricated InGaP/GaAs double junction cells bonded to (100)  $p^+$ -Si substrates using a similar process sequence.

A transmission electron microscope (TEM) image of a just-bonded GaAs/Si bonding interface and an interface after the subsequent annealing (400 °C, 1 min.) are shown in Figs. 2(a)

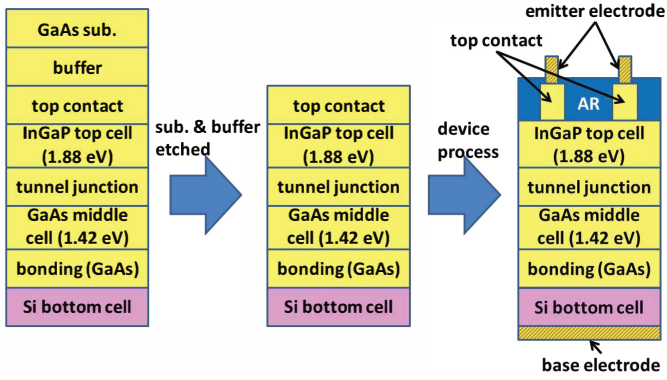


Fig. 1. The process sequence for fabricating hybrid triple-junction cells and their schematic layer structure.

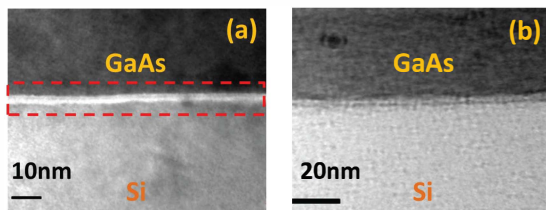


Fig. 2. A TEM image of (a) a just-bonded GaAs/Si interface, and (b) an interface after the subsequent annealing. (400 °C, 1 min.)

and 2(b), respectively. We confirmed that the GaAs bonding layer and Si substrates were firmly bonded even after the 400-°C annealing. We also found that a  $\approx 5$ -nm thick amorphous layer observed at the just-bonded interface vanished after the annealing, which suggests that the amorphous layer was recrystallized. Similar results were reported by another author [12].

### B. Cell Characterization

Performances of the fabricated cells were measured using an in-house solar simulator under the condition of air mass of 1.5G and one sun at room temperature. The current-voltage ( $J - V$ ) characteristics of the InGaP/GaAs/Si triple-junction and InGaP/GaAs double-junction cells are compared in Fig. 3. The mesa area of cells is a 2 mm by 2 mm square. Their short-circuit current ( $J_{SC}$ ), open circuit voltage ( $V_{OC}$ ), fill factor (FF), and the conversion efficiency are summarized in Table I. The conversion efficiencies of the triple-junction and double-junction cells are 24.4 and 18.4%, respectively. Separately fabricated Si cells revealed  $J_{SC}$  of  $\approx 35$  mA/cm<sup>2</sup> and  $V_{OC}$  of  $\approx 0.52$  V, respectively (not shown).

We measured characteristics of triple-junction cells with 1-mm by 1-mm and 2-mm by 2-mm mesas and those of double-junction cells with 1-mm by 1-mm, 2-mm by 2-mm, and 5-mm by 5-mm mesas.  $J_{SC}$  and  $V_{OC}$  values of the respective cells are shown in Fig. 4. Note that the difference in  $V_{OC}$  between the triple-junction and double-junction cells is approximately equal to  $V_{OC}$  of the Si cells, 0.52 V as cited above, irrespective

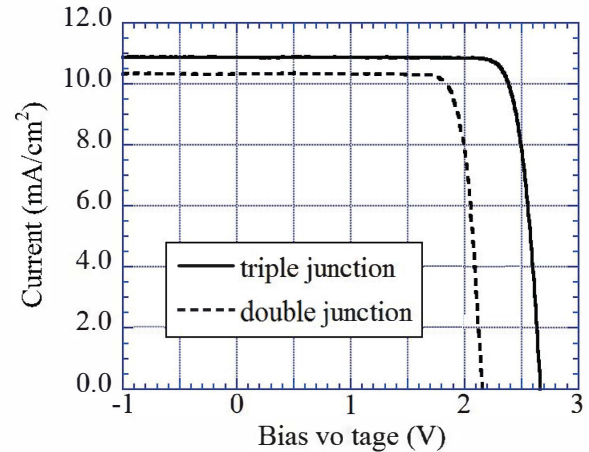


Fig. 3.  $J - V$  characteristics of a 2-mm by 2-mm InGaP/GaAs/Si hybrid triple-junction cell and a 2-mm by 2-mm InGaP/GaAs double-junction cell bonded to a  $p^+$ -Si substrate.

TABLE I  
PARAMETERS EXTRACTED FROM THE CELL CHARACTERISTICS.

Parameter	triple junction	double junction
$V_{OC}$ (V)	2.66	2.16
$J_{SC}$ (mA/cm <sup>2</sup> )	10.9	10.3
FF (%)	84.2	82.7
Efficiency (%)	24.4	18.4

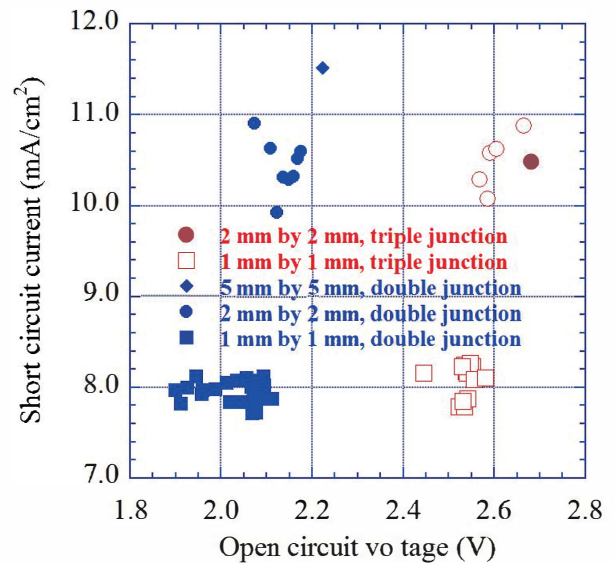


Fig. 4.  $J_{SC}$  and  $V_{OC}$  of InGaP/GaAs/Si triple-junction and InGaP/GaAs double-junction cells with different mesa areas.

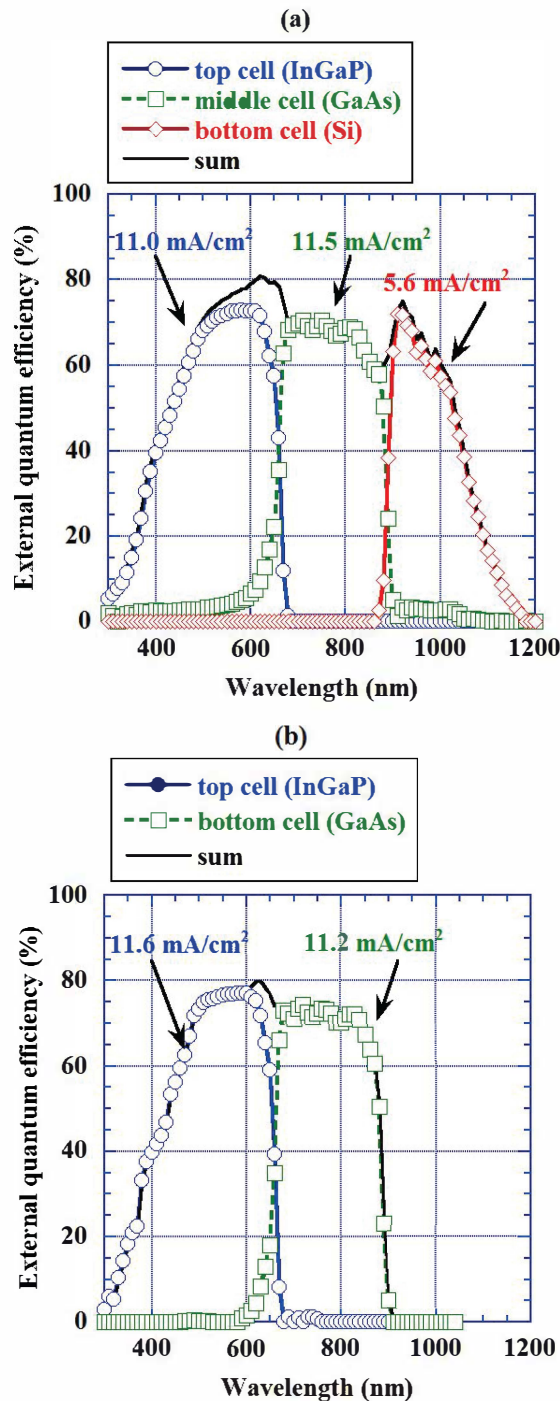


Fig. 5. EQE spectra of (a) a 2-mm by 2-mm InGaP/GaAs/Si hybrid triple-junction cell and (b) a 2-mm by 2-mm InGaP/GaAs double-junction cell bonded to a  $p^+$ -Si substrate. Estimated  $J_{SC}$  of each sub cell is also shown.

of their mesa area. We also find that  $J_{SC}$  in triple-junction cells is almost equal to that in double-junction cells with the same mesa areas. In addition  $J_{SC}$  in 2-mm by 2-mm cells,  $\sim 10$ – $11 \text{ mA/cm}^2$ , is approximately 1.3 times larger than that in 1-mm by 1-mm cells ( $\sim 8 \text{ mA/cm}^2$ ). A larger  $J_{SC}$  is observed for a 5-mm by 5-mm double junction cell. ( $11.5 \text{ mA/cm}^2$ )

We also measured spectral responses of 2-mm by 2-mm triple- and double-junction cells using Model QE-R (Enlitech). The probing light was focused on a  $\approx 1$ -mm by 1-mm area of the sample surface. Light emitting diodes were employed as sources of a bias light [21]. The spectra of external quantum efficiency (EQE) of the triple- and double-junction cells are shown in Figs. 5(a) and (b), respectively. The EQE spectra of InGaP- and GaAs-based sub cells in the triple-junction cells are close to their EQE spectra in the double-junction cells. We confirmed (not depicted) that the EQE of bottom cell in the triple-junction cell was similar to that of a single junction Si cell for wavelengths  $> 880 \text{ nm}$ .  $J_{SC}$  of the InGaP- and GaAs-based sub cells is estimated to be  $\approx 11$ – $12 \text{ mA/cm}^2$  by integrating the spectral responses. Obtained  $J_{SC}$  values are in agreement with the results of J-V measurements.  $J_{SC}$  of the Si-based sub cell is found to be  $5.6 \text{ mA/cm}^2$ .

The results of spectral response measurements suggest that performances of the triple-junction cell are limited by the characteristics of the bottom cell. The disagreement between this view and the finding from  $J - V$  measurements that  $J_{SC}$  in the triple-junction cell is close to that in the double-junction cell might be explained by the contention that the periphery of the Si-based bottom cell plays a certain role when the entire cells are illuminated in  $J - V$  measurements.

The portion of shaded areas in the III-V mesa, or the areas covered by either emitter electrodes or top contact layers, is 38.5, 20.4, and 12.6% in 1-mm by 1-mm, 2-mm by 2-mm, and 5-mm by 5-mm cells, respectively. The result that a lower  $J_{SC}$  was observed in a cell with a narrower mesa is, consequently, likely to be attributable to a larger shadow loss. Thus higher  $J_{SC}$  values, i.e., higher conversion efficiencies are assumed to be realized in cells with a smaller portion of shaded areas in mesas.

### III. CONCLUSION

We successfully fabricated InGaP/GaAs/Si hybrid triple junction cells by the surface activated bonding of a lattice-matched InGaP/GaAs double cell structure, which had been grown on a GaAs substrate in the reverse order, to a ion-implantation-based Si bottom cell structure and the selective etching of the GaAs substrate. The  $n^+$ -doped layer achieved by the ion implantation to Si worked as an emitter in the bottom cells and a part of the tunnel junction. The transmission electron microscope observation revealed that the GaAs/Si bonding interface was stable after the annealing at  $400 \text{ }^\circ\text{C}$ . A conversion efficiency of 24.4% was achieved in 2-mm by 2-mm square cells. The contribution of the periphery of the Si-based bottom cell was suggested. Higher efficiencies are assumed to be realized by lowering the shadow loss.

### ACKNOWLEDGEMENT

This work was partly supported by ‘‘Creative Research for Clean Energy Generation Using Solar Energy’’ project in Core Research for Evolutional Science and Technology (CREST) program of Japan Science and Technology Agency (JST).

## REFERENCES

- [1] [http://www.nrel.gov/ncpv/images/efficiency\\_chart.jpg](http://www.nrel.gov/ncpv/images/efficiency_chart.jpg).
- [2] M. Yamaguchi, T. Takamoto, K. Araki, N. E.-Daukes, "Multi-junction III-V solar cells: current status and future potential," *Solar Energy*, vol. 79, pp. 78-85, 2005.
- [3] J. F. Geisz, S. Kurtz, M. W. Wanlass, J. S. Ward, A. Duda, D. J. Friedman, J. M. Olson, W. E. McMahon, T. E. Moriarty, and J. T. Kiehl, "High-efficiency GaInP/GaAs/InGaAs triple-junction solar cells grown inverted with a metamorphic bottom junction," *Appl. Phys. Lett.* vol. 9, pp. 023502-1-023502-3, 2007.
- [4] F. Dimroth, et al. "Wafer bonded four-junction GaInP/GaAs/GaInAsP/GaInAs concentrator solar cells with 44.7% efficiency," *Prog. Photovolt: Res. Appl.* vol. 22, pp. 277-282 2014.
- [5] T. Soga, K. Baskar, T. Kato, T. Jimbo, and M. Umeno, "MOCVD growth of high efficiency current-matched AlGaAs/Si tandem solar cell," *J. Cryst. Growth*, vol. 174, pp. 579-584, 1997.
- [6] M. R. Lueck, C. L. Andre, A. J. Pitera, M. L. Lee, E. A. Fitzgerald, and S. A. Ringel, "Dual Junction GaInP/GaAs Solar Cells Grown on Metamorphic SiGe/Si Substrates With High Open Circuit Voltage," *IEEE Electron Device Lett.* vol. 27, no. 3, pp. 142-144, 2006.
- [7] M. J. Archer, D. C. Law, S. Mesropian, M. Haddad, C. M. Fetzer, A. C. Ackerman, C. Ladous, R. R. King, and H. A. Atwater, "GaInP/GaAs dual junction solar cells on Ge/Si epitaxial templates," *Appl. Phys. Lett.* vol. 92, pp. 103503-1-103503-3, 2008.
- [8] O. Moutanabbir and U. Gösele, "Heterogeneous Integration of Compound Semiconductors," *Annu. Rev. Mater. Res.* vol. 40, pp. 469-500, 2010.
- [9] Ph. Komninou, J. Stoemenos, G. P. Dimitrakopoulos, and Th. Karakostas, *J. Appl. Phys.* "Misfit dislocations and antiphase domain boundaries in GaAs/Si interface," *J. Appl. Phys.* vol. 75 pp. 143-152, 1994.
- [10] H. Takagi, K. Kikuchi, R. Maeda, T. R. Chung, and T. Suga, "Surface activated bonding of silicon wafers at room temperature," *Appl. Phys. Lett.* vol. 68, pp. 2222-2224, 1996.
- [11] H. Takagi, R. Maeda, T. R. Chung, N. Hosoda, and T. Suga, "Effect of Surface Roughness on Room-Temperature Wafer Bonding by Ar Beam Surface Activation," *Jpn. J. Appl. Phys.* vol. 37, pp. 4197-4203, 1998.
- [12] H. Takagi, R. Maeda, N. Hosoda, and T. Suga, "Transmission Electron Microscope Observations of Si/Si Interface Bonded at Room Temperature by Ar Beam Surface Activation," *Jpn. J. Appl. Phys.* vol. 38, pp. 1589-1594, 1999.
- [13] M. M. R. Howlader, T. Watanabe, and T. Suga, "Investigation of the bonding strength and interface current of p-Si/n-GaAs wafers bonded by surface activated bonding at room temperature," *J. Vac. Sci. Technol. B*, vol. 19, no. 6, pp. 2114-2118, 2001.
- [14] M. M. R. Howlader, T. Watanabe, and T. Suga, "Characterization of the bonding strength and interface current of p-Si/n-InP wafers bonded by surface activated bonding method at room temperature," *J. Appl. Phys.* vol. 91 pp. 3062-3066, 2002.
- [15] C. Wang, E. Higurashi, and T. Suga, "Void-Free Room-Temperature Silicon Wafer Direct Bonding Using Sequential Plasma Activation", *Jpn. J. Appl. Phys.* vol. 47, pp. 2526-2530, 2008.
- [16] N. Shigekawa, N. Watanabe, and E. Higurashi, "Electrical Properties of Si-based Junctions by SAB," in *Proc. 3rd Int. IEEE Workshop Low-Temperature Bonding for 3D Integration*, pp. 109-112, 2012.
- [17] J. Liang, T. Miyazaki, M. Morimoto, S. Nishida, and N. Shigekawa, "Electrical properties of Si/Si interfaces by using surface-activated bonding," *J. Appl. Phys.* vol. 114 pp. 183703-1-183703-6, 2013.
- [18] K. Derendorf, et al. "Fabrication of GaInP/GaAs/Si Solar Cells by Surface Activated Direct Wafer Bonding," *IEEE J. Photovoltaics*, vol. 3, no. 4, pp. 1423-1428, 2013.
- [19] J. Liang, T. Miyazaki, M. Morimoto, S. Nishida, N. Watanabe, and N. Shigekawa, "Electrical Properties of p-Si/n-GaAs Heterojunctions by Using Surface-Activated Bonding," *Appl. Phys. Express*, vol. 6, pp. 021801-1-021801-3, 2013.
- [20] N. Shigekawa, M. Morimoto, S. Nishida, and J. Liang, "Surface-activated-bonding-based InGaP-on-Si double-junction cells," *Jpn. J. Appl. Phys.* vol. 53, pp. 04ER05-1-04ER05-4, 2014.
- [21] E.H. Steenbergen, M.J. DiNezza, W.H.G. Dettlaff, S.H. Lim, and Y.-H. Zhang, "Effects of varying light bias on an optically-addressed two-terminal multicolor photodetector," *Infrared Phys. Technol.* vol. 54, pp. 292-295, 2011.